BIOINFORMATICS ORIGINAL PAPER

Vol. 27 no. 10 2011, pages 1404–1412
doi:10.1093/bioinformatics/btr158

Systems biology

Advance Access publication March 30, 2011

A qualitative continuous model of cellular auxin and

Martial Sankar[1,*], Karen S. Osmont[1], Jakub Rolcik[2], Bojan Gujas[1], Danuse Tarkowska[2], Miroslav Strnad[2], Ioannis Xenarios[3] and Christian S. Hardtke[1,*]

[1]Department of Plant Molecular Biology, University of Lausanne, CH-1015 Lausanne, Switzerland, [2]Laboratory of Growth Regulators, Palacky University and Institute of Experimental Botany Academy of Sciences of the Czech Republic, CZ-78371 Olomouc, Czech Republic and [3]Swiss Institute of Bioinformatics, CH-1015 Lausanne, Switzerland

Associate Editor: Alfonso Valencia

ABSTRACT

Motivation: Hormone pathway interactions are crucial in shaping plant development, such as synergism between the auxin and brassinosteroid pathways in cell elongation. Both hormone pathways have been characterized in detail, revealing several feedback loops. The complexity of this network, combined with a shortage of kinetic data, renders its quantitative analysis virtually impossible at present.

Results: As a first step towards overcoming these obstacles, we analyzed the network using a Boolean logic approach to build models of auxin and brassinosteroid signaling, and their interaction. To compare these discrete dynamic models across conditions, we transformed them into qualitative continuous systems, which predict network component states more accurately and can accommodate kinetic data as they become available. To this end, we developed an extension for the SQUAD software, allowing semi-quantitative analysis of network states. Contrasting the developmental output depending on cell type-specific modulators enabled us to identify a most parsimonious model, which explains initially paradoxical mutant phenotypes and revealed a novel physiological feature.

Availability: The package SQUADD is freely available via the Bioconductor repository at http://www.bioconductor.org/help/bioc-views/release/bioc/html/SQUADD.html.

Contact: martial.sankar@unil.ch; christian.hardtke@unil.ch

Supplementary information: Supplementary data are available at *Bioinformatics* online.

Received on September 16, 2010; revised on March 16, 2011; accepted on March 17, 2011

1 INTRODUCTION

The ontogenesis of plants is characterized by an intrinsic developmental plasticity, which reflects their capacity to adapt to environmental conditions and is frequently conveyed by modulation of plant hormone pathways (Nemhauser *et al.*, 2006). Thus, plant hormones are not only essential for various endogenous developmental programs, but also for the perception of, and adaptation to, environmental change. Several plant hormone pathways are known, and their often context-specific, overlapping activities suggest that they influence each other, sometimes in a hierarchical, sometimes in a synergistic manner. Auxin and brassinosteroids are among the best characterized hormones with well-defined signaling pathways and cellular effects. Both hormones are limiting for cell elongation, a process in which they act synergistically because of crosstalk between their pathways (Hardtke, 2007; Kuppusamy *et al.*, 2008).

A distinct feature that sets auxin apart from other plant hormones is the fact that it can be moved through the plant body by specialized molecular machinery. This regulated and directional transport, called polar auxin transport (PAT), contributes significantly to the local control of auxin action (Leyser, 2005). Although other hormones, including brassinosteroids (Savaldi-Goldstein *et al.*, 2007), might well be mobile within a certain range from their site of production, specialized transport systems apart from PAT have not been found so far. Together with auxin biosynthesis, PAT determines cellular auxin concentration, which is translated into a transcriptional response via the canonical auxin signaling pathway. This involves nuclear auxin receptors, transport inhibitor response 1 (TIR1) and homologs, a class of SCF-type E3 ubiquitin ligase F-box proteins that are activated by binding auxin, hence targeting transcriptional co-repressors of the auxin/indole-3-acetic acid (AUX/IAA) family for proteasome-mediated degradation (Dharmasiri *et al.*, 2005; Kepinski and Leyser, 2005). Since AUX/IAAs inhibit the activation potential of auxin response factors (ARFs), this releases ARFs to activate transcriptional targets of auxin signaling through auxin-responsive promoter elements (AuxREs) (Benjamins and Scheres, 2008).

Importantly, auxin signaling involves a negative feedback loop, as *AUX/IAA* genes are among the most prominent, early auxin signaling targets. Moreover, auxin signaling also affects PAT, because it controls the expression of several of the integral plasma membrane auxin efflux carriers, the PIN-FORMED (PIN) proteins (Sauer *et al.*, 2006; Vieten *et al.*, 2005; Wisniewska *et al.*, 2006). Therefore, auxin transport and signaling are intimately linked, and local auxin activity is conveyed by their interplay (Benjamins and Scheres, 2008; Leyser, 2005).

The brassinosteroid pathway represents a more classic signaling paradigm, where perception of the hormone at the plasma membrane modulates the activity of nuclear targets to eventually trigger gene expression changes (Kim *et al.*, 2009; Vert *et al.*, 2005). Brassinosteroids are perceived by integral

*To whom correspondence should be addressed.

plasma membrane proteins with a leucine-rich repeat receptor-like kinase topology, the brassinosteroid insensitive 1 (BRI1) and BRI1-like proteins. Binding of brassinosteroid promotes association of the receptors with another membrane-bound kinase, BRI1-associated receptor kinase 1, triggering a series of phosphorylation events. This signaling cascade, via several intermediates, inhibits the activity of BRASSINOSTEROID-INSENSITIVE 2 (BIN2), a glycogen synthase kinase 3/shaggy-like kinase. In the absence of brassinosteroid, BIN2 phosphorylates the highly homologous transcription factors bri1-EMS-SUPPRESSOR 1 (BES1) and BRASSINAZOLE RESISTANT 1 (BZR1). Thus, upon brassinosteroid signaling, aided by the phosphatase bri1-SUPPRESSOR 1 (BSU1), BES1 and BZR1 accumulate in a dephosphorylated state, which results in altered nucleo-cytoplasmic partitioning and DNA binding affinity towards brassinosteroid-responsive promoter elements (BRREs), and thus target gene activation. This signaling pathway involves a homeostatic feedback loop, since it directly impinges on brassinosteroid biosynthesis.

The pathways described above appear to be universally expressed throughout the plant, and have been implicated in many developmental or physiological processes. This is somewhat paradoxical, given that many of these processes do not appear to be related. However, while less variability has been observed in the brassinosteroid signaling pathway, (tissue-)specificity of auxin effects could be explained by the complexity of the auxin signaling components, notably the numerous *AUX/IAA* and *ARF* genes. The respective proteins are likely not fully redundant, thus their differential expression could introduce a cell type-specificity to auxin response (Weijers *et al*., 2005). Moreover, the ARF proteins do not only encompass transcriptional activators, but also transcriptional repressors. Another explanation could be that auxin, and brassinosteroid, action depends in part on molecular pre-patterns that could involve context-specific modulators and read-outs of auxin action (Badescu and Napier, 2006; Benjamins and Scheres, 2008; Braun *et al*., 2008; Strader *et al*., 2008; Tromas *et al*., 2009). One such modulator could be the *BREVIS RADIX* (*BRX*) gene, which is specifically expressed in the vasculature and is rate-limiting for auxin action, likely by impinging on brassinosteroid biosynthesis (Beuchat *et al*., 2010; Mouchel *et al*., 2006). As BRX activity is controlled by auxin at both the transcriptional and post-translational level (Scacchi *et al*., 2009), this suggests that *BRX* mediates crosstalk between the two hormone pathways, adding to accumulating evidence for a rate-limiting role of the brassinosteroid pathway in auxin response (Hardtke, 2007; Kuppusamy *et al*., 2008; Nemhauser *et al*., 2004; Vert *et al*., 2008). Another factor involved in auxin–brassinosteroid crosstalk is the repressive auxin response factor, ARF2, which has been shown to be a substrate of the BIN2 kinase (Vert *et al*., 2008) and thus a direct point of crosstalk between the two hormones.

Despite the detailed knowledge about the composition of the signaling pathways, their discrete output in a given context still remains largely obscure due to the quantitative nature of hormone signaling and the technical difficulty in measuring it. The best existing read-outs so far are (artificial) reporter genes, which allow some generic quantification of hormone pathway activity by response to endogenous transcription factors (Muller and Sheen, 2008; Sabatini *et al*., 1999). However, because of the multiple feedback loops in each pathway and a lack of quantitative data on the activity of individual components, e.g. the level and stability of transcripts and proteins, steady state signaling amplitude in a given condition and its developmental consequences are still nearly impossible to predict.

In an attempt to overcome these limitations, we sought to apply network modeling, which has proven useful in deciphering, sometimes paradoxical, experimental observations in *Arabidopsis* (e.g. Digiuni *et al*., 2008; Liu *et al*., 2010; Locke *et al*., 2006). We applied a Boolean logic approach (e.g. Pandey *et al*., 2010) to assess and analyze the auxin and brassinosteroid signaling networks, and their interaction. To compare the behavior of the network components across one or several conditions, we transformed a discrete dynamic model into a qualitative continuous system using the SQUAD software (Di Cara *et al*., 2007). This approach has been successfully applied previously to model gene regulatory networks (Philippi *et al*., 2009; Sanchez-Corrales *et al*., 2010). A comparison to alternative strategies ...(e.g., Diaz and Alvarez-Buylla, 2009) can be found in (Wittmann *et al*., 2009). Our model was able to explain various paradoxical experimental observations, thereby helping us to correctly place the *BRX* gene in the respective network and approximate how the cell type-specific expression of *BRX* could contribute to differential cell fate.

2 METHODS

2.1 Plant growth, genotyping and hormone measurements

The *Arabidopsis brx-2* and *arf2-8* null mutants used to create the double mutant have been described (Scacchi *et al*., 2009; Vert *et al*., 2008). Plant tissue culture, genotyping and auxin measurements were performed according to standard methods as described (Beuchat, *et al*., 2010; Sibout, *et al*., 2006).

2.2 Signaling network representation

To reconstruct the auxin and brassinosteroid pathways, literature information was used to assemble the signaling circuits with respect to the logical formalism and signaling network framework. As described (Klamt *et al*., 2006), signaling network models are structured by input, intermediate and output layers. The input represents the starting points of a signaling circuit, which formally are nodes without incoming arrows. Inversely, output nodes are circuit end points that can depict developmental or physiological output processes (Hyduke and Palsson, 2010). Together, the input and output layers define the boundaries for the intermediate layer, which represents the core signal transduction cascade. Due to their linear nature, signaling networks are prone to node reduction, which permits to decrease the complexity of the discrete analysis and avoid any delay issue during the analysis of the continuous form (Naldi *et al*., 2010). The network models were implemented using cellDesigner v4.0.1 (www.celldesigner.org). The model descriptions are available in XML format in the Supplementary Material.

2.3 Logical model simulation

Model simulations were performed using SQUAD v2.0 (Di Cara *et al*., 2007), which relies on a standardized qualitative dynamical systems method (Mendoza and Xenarios, 2006) to provide an ordinary differential equation (ODE) to each model component (Equation 1). This leads to the transformation of the original discrete step function into a sigmoid response curve. Each node's ODE relies on two parameters: the gain of the sigmoid, h, and the decay gi. In the absence of kinetic data, in this study we used the default values of $h = 10$ and $gi = 1$.

2.4 SQUAD add-on

An add-on to SQUAD developed for this study is provided as an R package named SQUADD (SQUad ADD-on) in the Supplementary Material. This add-on permits the generation of simulation matrices and prediction heat maps. Simulation matrices are useful to assess the individual node simulation profiles across several conditions (e.g. Supplementary Figure S1), whereas prediction heat maps are useful to analyze the node activation change between, e.g. a perturbed condition and a 'wild-type' condition (e.g. Fig. 5). The method takes the SQUAD simulation datasets as an input and interpolates the data points with a locally weighted smoothing line or least square fitting line. At a user-defined time value, the ratio of the interpolate values between two conditions can then be calculated. Finally, the color scale is defined according to the ratio range. In this study, we applied a lowess interpolation at $t=50$. The SQUADD software including a tutorial can be downloaded as a Bioconductor package at http://www.bioconductor.org/help/bioc-views/release/bioc/html/SQUADD.html.

3 RESULTS

3.1 Modeling the core of cellular auxin perception

The goal of our study was to develop a cellular model for auxin–brassinosteroid interaction in cell elongation. Roots grow at their tips, where an apical meristem that harbors stem cells continuously produces new cells that undergo a stage of proliferation, followed by elongation and eventually differentiation (Osmont *et al*., 2007). Both auxin and brassinosteroids are limiting in this process. To build up our core models of the auxin and brassinosteroid pathways, we relied on solid, well-established experimental data from the literature as summarized in recent reviews (Benjamins and Scheres, 2008; Hardtke, 2007; Kieffer *et al*., 2010; Kim and Wang, 2010; Scheres and Xu, 2006; Vert *et al*., 2005). An overview of these regulatory interactions can be found in Supplementary Table S1. We started by creating a model of the core auxin signaling loops, which includes the AUX/IAA transcriptional repressors, the TIR1-type auxin receptors and the ARF transcriptional activators. As a generic developmental read-out of the model we defined auxin-responsive elements and thus genes that are controlled by ARF activity, including *AUX/IAA* genes as well as *PIN* genes. Finally, auxin itself was added as a continuous stimulus in the model, based on the observation that shoot-derived auxin is transported towards the root tip from cell to cell via PAT during seedling development. Evacuation of auxin from the cell by PIN proteins was integrated into the model as a negative effect of PINs on cellular auxin activity.

3.1.1 Modeling strategy Due to the absence of quantitative data for most of the signaling components and the inherent difficulty to obtain such, ideally kinetic data at spatio-temporal resolution in a developmental context, we analyzed the signaling network by a Boolean formalism approach (i.e. a logical model). In a Boolean formalism, each node (i.e. model component) is defined by a variable x, which represents its state of activation ($x=1$) or inactivation ($x=0$). The state of each node depends on its interaction or regulatory relationship with other nodes. By extension, the activation state of the system (i.e. of the totality of nodes) is given by the vector of size n ($n=$number of nodes) of the node activation states. Starting from given initial conditions and in response to a stimulus (in our models auxin and/or brassinosteroids), this vector is then updated synchronously or asynchronously, until the system reaches a stable, or oscillating (complex) steady state.

Boolean formalism is powerful but not very intuitive as the range of values is discrete and kinetics are not considered, i.e. the time scale is arbitrary. Components can be updated synchronously or asynchronously, however synchronous update of the vector is most of the time unrealistic, because it would assume that the components are activated or inhibited simultaneously. This is not the case in biological systems, where components are activated or inhibited on different time scales that depend on the kinetics of individual interactions (e.g. affinity in protein–protein interactions) or the speed of the activation/inhibition process (e.g. transcription versus translation or protein degradation). To overcome the lack of time scales in the Boolean approach, computational tools have been developed, such as the SQUAD software, in which vector updates are entirely asynchronous (Di Cara *et al*., 2007). For example, in a given sequence of A activates B activates C, a change of state in A only triggers a change of state in B with a certain delay. A change of state in C will then again only follow with a delay after the state of change in B. Moreover, SQUAD permits assessment of the behavior of components across an arbitrary time scale. This is because SQUAD transforms a classic dynamic Boolean model into a continuous one by using ordinary differential equations, one for each node, given by the following equation:

$$\frac{dx_i}{dt} = \frac{-e^{0.5h} + e^{-h(w_t)}}{(1-e^{0.5h})(1+e^{-h(w_i-0.5)})} - g_i x_i$$

With this equation, intermediate values between 0 and 1 and therefore sigmoid curves can be obtained, which are useful to assess the behavior of components. The h parameter accounts for the sigmoid gain, i.e. it controls the steepness of the curve (high values will give curves close to a step function). gi represents the decay of the node. wi is the continuous form of the truth table of each node, i.e. the combinatorial effect of all the inputs into a given node. Due to lack of kinetic information, the computations in our models were performed with the default values of h = 10 and gi = 1. It is important to note however, that kinetic data that should eventually become available could be easily integrated into our models by setting h and gi parameters accordingly, allowing model refining. The logic rules and equations describing the nodes of all models presented in this study can be found in the Supplementary Material.

3.1.2 Behavior of the core SCFTir1-AUX/IAA-ARF auxin perception module Based on the experimental data and strategy outlined above, we created a model for the core auxin perception machinery (Fig. 1A), which can be handled like a circuit. A signal is injected into the system via an input node and its route can be followed through the OR/AND gates and the node state switches until it is caught by the terminal output node. The biological signal for our model is auxin, which was thus set as the initial stimulus. This auxin stimulation node represents the events of both passive and active auxin influx. As the ultimate output of the model, we defined a generic 'elongation growth' node, which represents the developmental output of altered auxin-responsive gene expression on cell elongation. Finally, the tendency of the activation pattern of each node can be represented by a linear regression, which permits a numerical estimation of node behavior (see below).

The SQUAD analysis indicates that the network components exhibit oscillatory behavior (Fig. 1B), including the elongation output, which is revealed by the sigmoid feature of the program. This result is consistent with the idea of inherent buffering in signaling

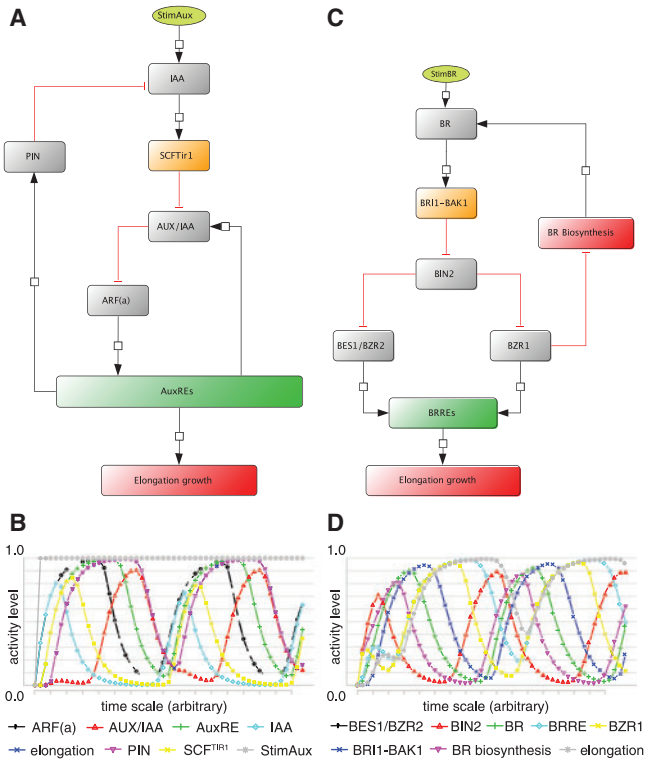

Fig. 1. The auxin and brassinosteroid signaling network models. (**A**) Network representation of the auxin signaling core. (**B**) Simulation output of the network presented in (A) after transformation into a qualitative continuous system using SQUADD (initial continuous auxin stimulation xIAA = 1, initial node states $x = 0$). (**C**) Network representation of the brassinosteroid signaling core. (**D**) Simulation output of the network presented in (C) after transformation into a qualitative continuous system using SQUADD (initial node states $x = 0$).

networks, which prevents a signaling lock-in as well as exaggerated response to transient stimulus and thus provides developmental flexibility. As SCFTIR1 is activated by auxin, Aux/IAAs are inhibited, allowing ARFs to reach their maximum activity, while decreasing SCFTIR1 activity stabilizes Aux/IAAs and thus inhibits ARFs. Importantly, to avoid a lock-in steady state of the network, negative feedback on auxin through PAT is required, which is mediated by the positive effect of auxin perception on PIN activity. In summary, the model correctly simulates the behavior of the core components in auxin perception. Due to the solid experimental evidence for the functioning of the auxin perception machinery, we considered the behavior of its components as a control in the analyses of subsequent, more complex models.

3.2 Modeling of brassinosteroid signaling and its interaction with auxin signaling

In the next step, we sought to extend our model by integrating the brassinosteroid signaling pathway and thus account for the observed synergism between the two hormone pathways (Hardtke, 2007; Kuppusamy *et al*., 2008; Mouchel *et al*., 2006; Nemhauser *et al*., 2004). First, similar to the auxin model, we built a model of brassinosteroid signaling based on experimental data from the literature (Kim *et al*., 2009; Kim and Wang, 2010; Vert *et al*., 2005) (Fig. 1C). Beyond the signal transduction from BRI1 to the BES1/BZR1 transcription factors and the eventual modulation of brassinosteroid-responsive gene expression, we also included an explicit feedback on brassinosteroid biosynthesis. This feedback is not only an important component of brassinosteroid homeostasis, but also the major dampening factor of the signaling pathway, conceptually similar to AUX/IAA feedback on auxin signaling. In response to a brassinosteroid stimulus, this model again swiftly reaches a quasi-steady state, including an oscillating developmental output (Fig. 1D). Thus, both of our models appear to correctly capture the signaling features described in the literature.

3.2.1 Auxin–brassinosteroid interaction—the ARF2 connection

To integrate the two models, auxin- and brassinosteroid-responsive gene expression was linked to a common developmental output node, reflecting the observed synergism of the two hormones in controlling cell elongation (Hardtke, 2007; Nemhauser *et al*., 2004; Wang *et al*., 2005). Thus, in the integrated model, the developmental output reports the impact of both auxin- and brassinosteroid-responsive promoter elements, which are indeed frequently found together in genes that respond to both hormones.

Beyond the common occurrence of auxin- and brassinosteroid-responsive elements in promoters, only few components that might mediate more direct, non-genomic auxin–brassinosteroid interaction have been described, such as the inhibitory ARF2. ARF2 activity is directly modulated through the BIN2 kinase, which can phosphorylate ARF2 to prevent it from DNA binding (Vert *et al*., 2008). Thereby brassinosteroids would activate an inhibitory component of auxin signaling, since all ARFs can bind to the same auxin-responsive promoter elements (Guilfoyle and Hagen, 2007). Moreover, a significant effect of ARF2 on genes involved in auxin biosynthesis has been reported, suggesting that brassinosteroid might modulate auxin biosynthesis (Vert *et al*., 2008). However, the contribution of cellular auxin biosynthesis to our model is negligible for the developmental output as long as auxin flow through the cell is maintained by PAT, which is consistent with established models and experimental findings (Grieneisen *et al*., 2007). Based on these reported results, we placed ARF2 as a central node connecting auxin and brassinosteroid signaling in our model (Fig. 2A). Moreover, we also integrated ARF2 into the auxin signaling pathway, because inhibitory ARFs, just like activating ones, do interact with AUX/IAA proteins, although at seemingly lower affinity (Tiwari *et al*., 2003).

The exact role of inhibitory ARFs (ARFi) is not clear, and it has been suggested that they could act by competing with activating ARFs (ARFa) for binding sites, or by directly inhibiting them upon dimerization (Guilfoyle and Hagen, 2007). For our logical model, this is directly not relevant as either mode of interaction impinges on kinetic parameters, but not the logic. In our model, we placed ARF2 under AUX/IAA control, such that AUX/IAA degradation in response to auxin stimulus would remove one level of inhibition from ARFi. Notably, however, in our logical model the exact mode of ARF2 inhibition does not matter for the working of the auxin core perception module, i.e. the quasi-steady state behavior is similar, although the (unknown) signaling amplitude might differ with or without ARFi. For the integrated model, again an oscillating quasi-steady state developmental output was observed, however with a slightly more restricted amplitude (Fig. 2B).

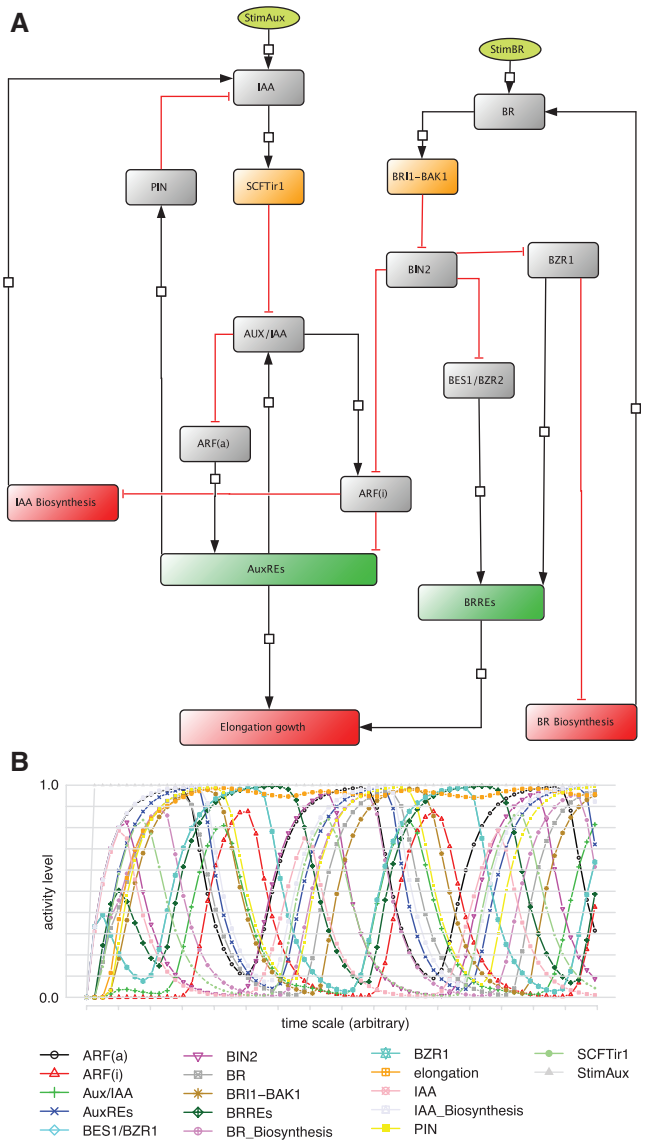

Fig. 2. Interaction between auxin and brassinosteroid signaling through ARF2. (**A**) Network representation of the integrated pathways connecting auxin and brassinosteroid signaling through the crosstalk component ARF2. (**B**) Simulation output of the network presented in (A) after transformation into a qualitative continuous system using SQUAD (continuous auxin stimulation xIAA = 0, initial node states $x = 0$).

3.2.2 Auxin–brassinosteroid interaction—integration of BRX A subject of special interest to us was to integrate the *BRX* gene into our model, since its position with respect to auxin and brassinosteroid signaling remains obscure despite the experimental evidence collected so far (see above). In particular, we aimed to evaluate a suspected role of *BRX* in an accessory auxin signaling pathway, which could serve to modulate auxin-response in a context-dependent manner (Scacchi *et al*., 2009).

To place *BRX* in our model, we first considered the regulatory influence of auxin on *BRX* activity. The *BRX* promoter contains prototypical AuxREs, and consistently, *BRX* expression is highly auxin-inducible, presumably through the canonical auxin signaling core (Mouchel *et al*., 2006; Scacchi *et al*., 2009). At the same time, auxin has a more direct effect on BRX protein, by promoting its transfer into the nucleus, where it presumably regulates transcription in conjunction with NGATHA (NGA) B3-type transcription factors (Scacchi *et al*., 2009). Thus, we placed *BRX* directly under auxin control. This regulation was considered as activating, although the nuclear transfer of BRX eventually results in BRX degradation (Scacchi *et al*., 2009). The latter would only restrict the duration of nuclear BRX activity, however, which can be neglected in a logical model.

The positive regulation of *BRX* by auxin, both at the transcriptional and post-translational level, would not influence the developmental output unless *BRX* activity feeds back into the network. This feedback is assumed to pass through the brassinosteroid pathway, possibly by promoting brassinosteroid biosynthesis, since *brx* phenotypes can be largely rescued by brassinosteroid application (Mouchel *et al*., 2006), and since gain-of-function lines constitutively and ectopically over-expressing full length BRX or a stabilized, partially active C-terminal fragment contained significantly higher levels of the major active brassinosteroids, brassinolide and its precursor, castasterone (Beuchat *et al*., 2010). Therefore, a positive influence of *BRX* on brassinosteroid biosynthesis was included in our model (Fig. 4A).

Finally, we also included the interaction of activated (nuclear localized) BRX with NGA transcription factors into our model, since the latter have been proposed to positively regulate auxin biosynthesis (Trigueros, *et al*., 2009). Whether BRX has an inhibitory or an activating influence on NGA remains to be experimentally determined. However, for our model this was not relevant, because as stated above, as long as auxin is provided by PAT, cellular auxin biosynthesis is negligible for the developmental output.

Different variants of the full model (i.e. including ARF2, BRX and NGA1) were created (Fig. 4A; Table 1) to account for the unknowns described above, such as the regulatory relation between BRX and NGA1. Moreover, we also created variants that assumed a potential direct influence of *BRX* on auxin-responsive gene expression (Scacchi *et al*., 2009). Only variants with a valid (i.e. steady state) developmental output were retained for further analysis (variants 4.1.1, 4.2.1, 5.1.1 and 5.2.1; Table 1) (Supplementary Fig. 1). Developmental output that could not reach a steady state any longer and fluctuated in a stochastic manner was observed if the positive link between *BRX* and brassinosteroid biosynthesis was removed, reinforcing its significance.

3.3 Behavior and testing of the integrated models

Similar to the previous model, the extended versions produced an oscillating quasi-steady state developmental output in most variants (Fig. 4B). This output displayed different trajectories however, consistent with the idea that accessory factors can introduce differential cell fate (Fig. 4B). We would like to note that the cyclic attractors (i.e. oscillating steady states) are consistent with various experimentally observed feedbacks, for instance the transcriptional re-activation of *AUX/IAAs* in response to their auxin-mediated degradation and the associated oscillation of auxin response. Whether other component states predicted to oscillate by our models in fact do so, for instance hormone levels, is not known and experimentally challenging to determine. Dynamic reporters that can

Table 1. Hierarchical summary view of the different models generated and tested in this study

Model version	Description	No. of nodes	No. of edges	Feedbacks ±(−)	Developmental output valid?
1	Auxin core model	8	9	2 (1)	Yes
2	BR core model	8	9	1 (0)	–
3	Integrated auxin-BR model	18	24	4 (1)	–
	Add BRX	/	/	/	/
4	IAA activates BRX	20	28	5 (1)	–
4.1	BRX activates NGA1	20	29	6 (1)	–
4.1.1	BRX activates BR biosynthesis	20	29	6 (1)	Yes
4.1.2	BRX inhibits BR biosynthesis	20	29	6 (1)	No
4.2	BRX inhibits NGA1	20	29	6 (1)	–
4.2.1	BRX activates BR biosynthesis	20	29	6 (1)	Yes
5	IAA activates BRX activates ARF(a)	20	29	5 (1)	–
5.1	BRX activates NGA1	20	30	6 (1)	–
5.1.1	BRX activates BR biosynthesis	20	30	6 (1)	Yes
5.1.2	BRX inhibits BR biosynthesis	20	30	6 (1)	No
5.2	BRX inhibits NGA1	20	30	6 (1)	–
5.2.1	BRX activates BR biosynthesis	20	30	6 (1)	Yes
6	BRX activates AuxRE	20	30	6 (1)	No
7	BRX inhibits Aux/IAA	20	30	6 (1)	No

be followed by live imaging at high temporal and cellular resolution would be required for this purpose. We would like to highlight however that modified logical rules can be found to eliminate cyclic attractors in our model if justified, and that our model describes an abstracted signaling network rather than, for instance, a gene regulatory network. Even if the steady states emerging from our models are oscillatory, they clearly describe the difference between the perturbated conditions.

In the next step, we aimed to test whether the models accurately reflect observed experimental findings. First, we perturbed the models by removing *BRX* a short time after stimulation (Fig. 4C). This resulted in dramatically altered developmental output, which even reached a linear steady state close to inactivity as compared to the full model in two variants (5.1.1 and 5.2.1). By contrast, removing *ARF2* from the model did not have any major effect on the developmental output. Both results match with the severity of the root growth phenotypes of the respective mutants, i.e. the strong short root phenotype of *brx* versus absence of a morphological root phenotype in *arf2* (Mouchel *et al*., 2004; Vert *et al*., 2008).

Finally, we tested whether the developmental output of our model could be rescued by a brassinosteroid stimulus after a loss of *BRX* function, simulating the phenotypic rescue of *brx* mutants by brassinosteroid application (Mouchel *et al*., 2006). This was indeed the case, i.e. adding brassinosteroid stimulus to the model after elimination of *BRX* activity and subsequent breakdown of

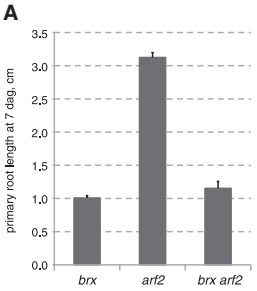

B

hormone content in pmol per g fresh weight

genotype	replicate	IAA	IAA-Asp	IAA-Glu	IAM
Sav-0	1	178	4.8	3.3	65
	2	150	4.9	2.6	79
	3	176	5.3	2.8	82
brx^{S}	1	215	8.6	6.8	50
	2	228	11.1	6.1	37
	3	241	13.2	6.0	52
35S::BRX^{CT} in *brx*^{S} g.o.f.	1	119	11.7	5.6	41
	2	123	11.2	6.4	44
	3	128	-	6.9	43
35S::BRX in *brx*^{S} g.o.f.	1	174	6.7	4.2	92
	2	186	6.4	3.8	99
	3	182	6.8	3.9	88

Fig. 3. Auxin content in *brx* mutants and root growth phenotypes. (**A**) Primary root growth in wild-type, *brx* mutant, *arf2* mutant and *brx arf2* double mutant seedlings in tissue culture. (**B**) Free auxin (IAA), auxin conjugate (IAA-Asp, IAA-Glu) and auxin precursor (IAM) content of *brx* mutant seedlings (*brxS*), their wild-type background (Sav-0) and gain-of-function lines obtained from ectopic over-expression of the BRX C-terminus (BRX^{CT}) or full length BRX.

developmental output swiftly restored the output to a pattern that was largely similar to the unperturbed model (Fig. 4D). Interestingly, this was only possible if *BRX* was not positioned within the brassinosteroid signal transduction module.

3.3.1 Testing the model - genetic interaction between ARF2 and BRX Experimental support for the notion that *BRX* does not fit into the brassinosteroid signaling chain was obtained from the analysis of *arf2 brx* double mutants. Previously, it was found that the *long hypocotyl 5 (hy5)* mutation significantly suppresses the *brx* root growth phenotype in *brx hy5* double mutants (Scacchi *et al*., 2009). Supposedly, this is due to constitutively increased auxin-responsive transcription as conferred by *hy5* loss of function (Sibout *et al*., 2006), which can in turn offset diminished auxin-responsiveness in *brx* mutants to some degree. Along these lines, it was speculated that quantitatively impaired auxin-response in *brx* mutants might be compensated by *arf2* mutation. To test this hypothesis, we generated an *arf2 brx* double mutant from respective null alleles. Assessment of the root growth phenotype of this double mutant revealed that it was not significantly different from the *brx* control line (Fig. 3A). Thus, the *arf2* mutation cannot suppress the effect of *brx*, which is consistent with perturbation of our models, i.e. the developmental output after removal of *BRX* and *ARF2* activity from the model was identical to the output observed after *BRX* removal only (Fig. 4E). This finding, together with the brassinosteroid rescue of *brx* phenotypes, would also suggest that the main point of auxin–brassinosteroid synergism at the transcriptional level are genes that are activated by both AuxREs and BRREs in their promoters.

3.3.2 Semi-quantitative presentation of perturbation consequences by predictive heat maps In the next step, we aimed to determine which of the integrated models best accommodate additional experimental data. To facilitate this task, we generated predictive heat maps to assess the activity state change of components between a perturbation and the normal condition. As SQUAD uses an exponential interpolation of Boolean states to obtain continuous activation values, and since activation states do not really represent quantitative experimental data, an absolute quantitative prediction of component activities is not possible. However, a relative, semi-quantitative analysis can be performed to reflect a qualitative change

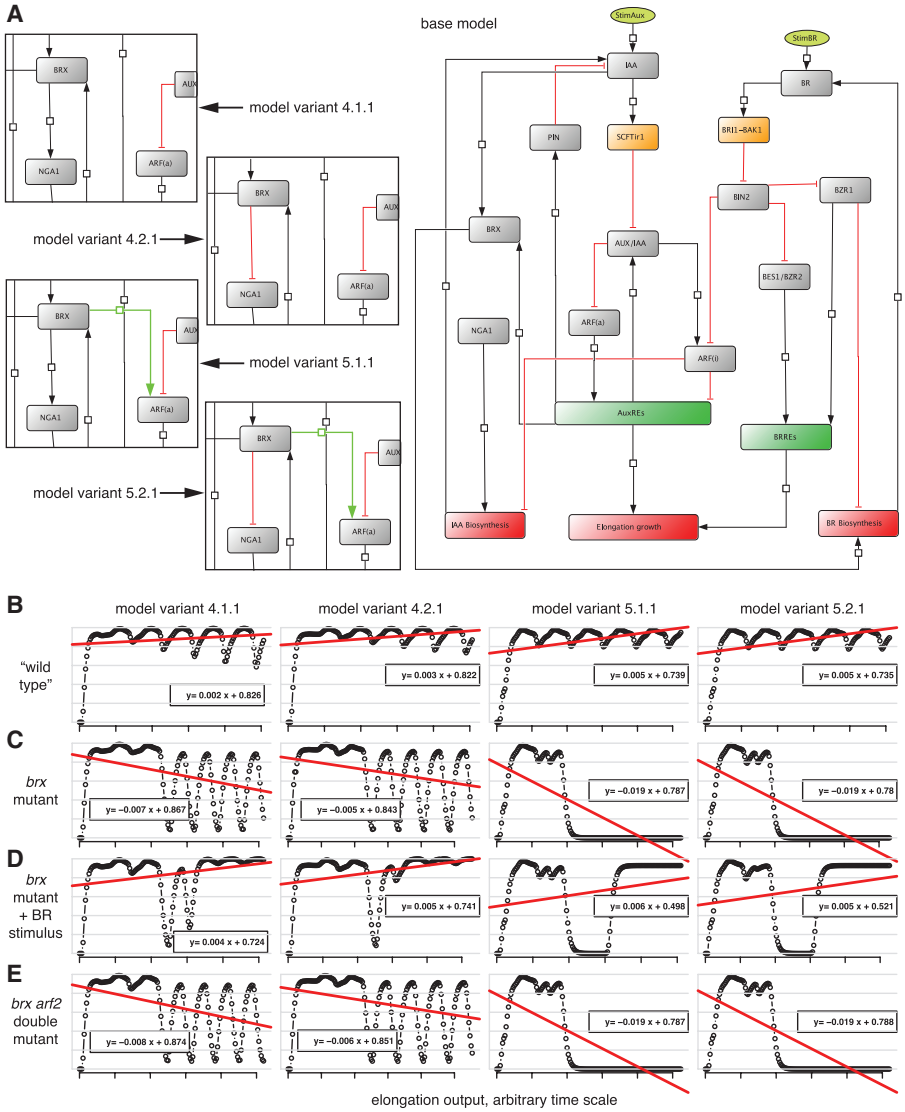

Fig. 4. Alternative integration of BRX into the network model. (**A**) Extended model of auxin–brassinosteroid interaction after integration of BRX and NGA1. Model variants that result in valid (i.e. coherent) developmental output throughout perturbed conditions are indicated. (**B**) Developmental output response curve of the different model variants over an arbitrary time scale (black), with the least square regression (red) indicated (continuous auxin stimulus $x = 1$). (**C**) Developmental output response curve after inactivation of BRX (xBRX coerced to 0 at $t = 13$). (**D**) Developmental output response curve after inactivation of BRX (xBRX coerced to 0 at $t = 13$) and rescue by brassinosteroid stimulus (continuous BR stimulus xBR = 0.4 at $t = 25$). (**E**) Developmental output response curve after inactivation of BRX (xBRX coerced to 0 at $t = 13$), followed by inactivation of ARF2 (xARFi coerced to 0 at $t = 25$).

in behavior of components between any two conditions. For such an evaluation, we implemented an R-based script to generate predictive heat maps using a simple algorithm (see Supplementary Material, SQUAD add-on R package). This tool takes the SQUAD simulation datasets as an input and interpolates the various data points for components with a locally weighted smoothing line at a user-defined time value. To compare two model variants, it then calculates the ratio of the interpolated values for a given component between a perturbation and the normal condition. Integrated across the time scale, this then indicates a relative change in the activity status of a node, i.e. an overall increase or decrease in activity. Finally, this relative change is then presented in a color scale grid, permitting intuitive assessment of the consequences of model perturbations and variations (Fig. 5).

Starting from our set of model variants, we generated predictive heat maps to compare the relative node states for the perturbations described above. We then determined for which variant model the experimental observations in the *brx* mutant fit best, focusing on two key results: (i) the observation that the expression of an AuxRE reporter gene is reduced in *brx* roots (Mouchel *et al.*, 2006); (ii) the observation that *brx* roots mimic wild-type roots treated with auxin transport inhibitors (Scacchi *et al.*, 2009), consistent with a downregulation of certain *PIN* genes in *brx* (Mouchel *et al.*, 2006); Only models 5.1.1 and 5.2.1 matched these observations.

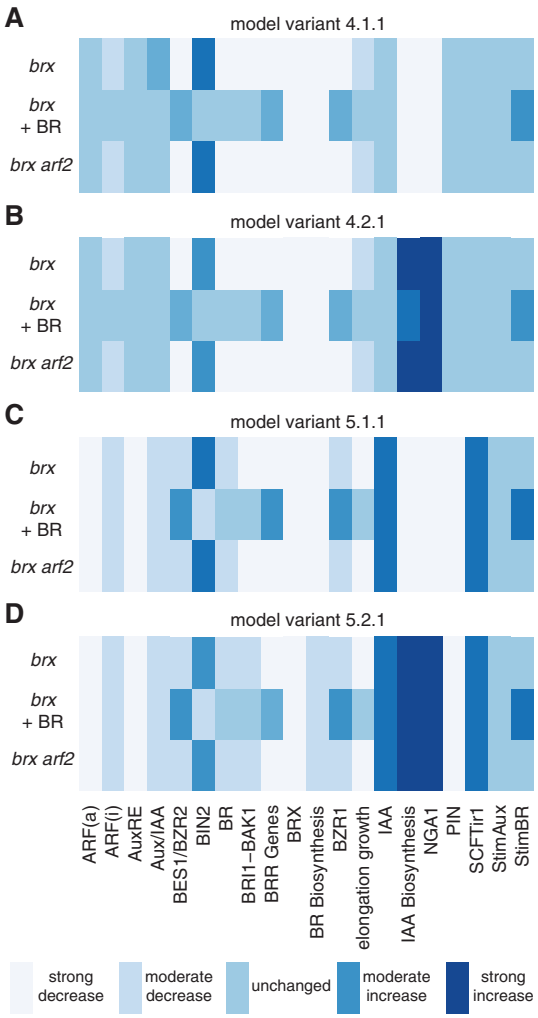

Fig. 5. Semi-quantitative evaluation of model output by predictive heat maps. (**A**–**D**) Predictive heat maps of relative changes of node activities in the model variants and perturbations as described in Figure 4, in comparison to the respective unperturbed models.

The principal difference between these two models is in the regulatory relationship between BRX and NGA1, which is reflected in a predicted decrease (5.1.1) or increase (5.2.1) in auxin biosynthesis and thus free auxin levels upon *BRX* loss of function. Surprisingly, direct measurement indicated that free auxin levels are indeed significantly increased in *brx* seedlings (Fig. 3B), suggesting that model 5.2.1 is most parsimonious with experimental observations.

To further evaluate the robustness of our model, we also ran it in Boolean, synchronous mode using the GinSim software (Gonzalez *et al*., 2006), which confirmed the cyclic attractors observed in the continuous form (see Supplementary Material). Finally, we also conducted a stability analysis by sampling a range of parameter values and time points. This analysis corroborated earlier findings about sensible parameter ranges (Mendoza and Pardo, 2010) and revealed very little variation in the qualitative behavior of our model, confirming that it is robust (see heat maps in the Supplementary Material).

3.4 Conclusions

In summary, we have built qualitative and continuous logical models of auxin and brassinosteroid signaling, and their interaction. The models account for well established as well as novel experimental observations and demonstrate how a cell type-specific modulator, *BRX*, could be integrated. Taking into account novel experimental data also allowed us to choose between alternative models to correctly place *BRX* in the network. This most parsimonious model predicts an inhibition of NGA1 by BRX and an accessory role of BRX in auxin perception and signaling, guiding future experimentation. Notably, no valid developmental output was observed when a direct or indirect (e.g. through NGA1), but ARF-independent impact of *BRX* on AuxREs was assumed. The recent experimental confirmation that BRX can interact directly with ARFs was in fact motivated by this prediction (Scacchi *et al*., 2010). Finally, our models can serve as a basis for the work of others and, thanks to the SQUAD approach, can be extended for quantitative, kinetic data as they become available.

ACKNOWLEDGEMENTS

We would like to thank Dr J. Nemhauser for *arf2* seeds. M.S. performed the modeling and the development of SQUAD add-ons. K.S.O. and B.G. generated and analyzed *arf2 brx* mutants. J.R. and D.T. performed hormone measurements. M.S., I.X. and C.S.H. designed the research and wrote the article together with M.S.

Funding: Swiss National Science Foundation SystemsX 'Plant growth in a changing environment' project.

Conflict of Interest: none declared.

REFERENCES

Badescu,G.O. and Napier,R.M. (2006) Receptors for auxin: will it all end in TIRs? *Trends Plant Sci.*, **11**, 217–223.

Benjamins,R. and Scheres,B. (2008) Auxin: the looping star in plant development. *Annu. Rev. Plant Biol.*, **59**, 443–465.

Beuchat,J. *et al*. (2010) BRX promotes Arabidopsis shoot growth. *New Phytol.*, **188**, 23–29.

Braun,N. *et al*. (2008) Conditional repression of AUXIN BINDING PROTEIN1 reveals that it coordinates cell division and cell expansion during postembryonic shoot development in Arabidopsis and tobacco. *Plant Cell*, **20**, 2746–2762.

Dharmasiri,N. *et al*. (2005) The F-box protein TIR1 is an auxin receptor. *Nature*, **435**, 441–445.

Diaz,J. and Alvarez-Buylla,E.R. (2009) Information flow during gene activation by signaling molecules: ethylene transduction in Arabidopsis cells as a study system. *BMC Syst. Biol.*, **3**, 48.

Di Cara,A. *et al*. (2007) Dynamic simulation of regulatory networks using SQUAD. *BMC Bioinformatics*, **8**, 462.

Digiuni,S. *et al*. (2008) A competitive complex formation mechanism underlies trichome patterning on Arabidopsis leaves. *Mol. Syst. Biol.*, **4**, 217.

Gonzalez,A.G. *et al*. (2006) GINsim: a software suite for the qualitative modelling, simulation and analysis of regulatory networks. *Biosystems*, **84**, 91–100.

Grieneisen,V.A. *et al*. (2007) Auxin transport is sufficient to generate a maximum and gradient guiding root growth. *Nature*, **449**, 1008–1013.

Guilfoyle,T.J. and Hagen, G. (2007) Auxin response factors. *Curr. Opin. Plant. Biol.*, **10**, 453–460.

Hardtke,C.S. (2007) Transcriptional auxin-brassinosteroid crosstalk: who's talking? *Bioessays*, **29**, 1115–1123.

Hyduke,D.R. and Palsson,B.O. (2010) Towards genome-scale signalling-network reconstructions. *Nat. Rev. Genet.*, **11**, 297–307.

Kepinski,S. and Leyser, O. (2005) The Arabidopsis F-box protein TIR1 is an auxin receptor. *Nature*, **435**, 446–451.

Kieffer,M. *et al*. (2010) Defining auxin response contexts in plant development. *Curr. Opin. Plant. Biol.*, **13**, 12–20.

Kim,T.W. *et al*. (2009) Brassinosteroid signal transduction from cell-surface receptor kinases to nuclear transcription factors. *Nat. Cell. Biol.*, **11**, 1254–1260.

Kim, T.W. and Wang, Z.Y. (2010) Brassinosteroid signal transduction from receptor kinases to transcription factors. *Annu. Rev. Plant Biol.*, **61**, 23.21–23.24.

Klamt,S. *et al*. (2006) A methodology for the structural and functional analysis of signaling and regulatory networks. *BMC Bioinformatics*, **7**, 56.

Kuppusamy,K.T. *et al*. (2008) Cross-regulatory mechanisms in hormone signaling. *Plant Mol. Biol.*, **69**, 375–381.

Leyser,O. (2005) Auxin distribution and plant pattern formation: how many angels can dance on the point of PIN? *Cell*, **121**, 819–822.

Liu,J. *et al*. (2010) Modelling and experimental analysis of hormonal crosstalk in Arabidopsis. *Mol. Syst. Biol.*, **6**, 373.

Locke,J.C. *et al*. (2006) Experimental validation of a predicted feedback loop in the multi-oscillator clock of Arabidopsis thaliana. *Mol. Syst. Biol.*, **2**, 59.

Mendoza,L. and Pardo,F. (2010) A robust model to describe the differentiation of T-helper cells. *Theory Biosci*., **129**, 283–293.

Mendoza,L. and Xenarios,I. (2006) A method for the generation of standardized qualitative dynamical systems of regulatory networks. *Theor. Biol. Med. Model.*, **3**, 13.

Mouchel,C.F. *et al*. (2004) Natural genetic variation in Arabidopsis identifies BREVIS RADIX, a novel regulator of cell proliferation and elongation in the root. *Genes Dev*., **18**, 700–714.

Mouchel,C.F. *et al*. (2006) BRX mediates feedback between brassinosteroid levels and auxin signalling in root growth. *Nature*, **443**, 458–461.

Muller,B. and Sheen,J. (2008) Cytokinin and auxin interaction in root stem-cell specification during early embryogenesis. *Nature*, **453**, 1094–1097.

Naldi,A. *et al*. (2010) Diversity and plasticity of Th cell types predicted from regulatory network modelling. *PLoS Comput. Biol.*, **6**, e1000912.

Nemhauser,J.L. *et al*. (2006) Different plant hormones regulate similar processes through largely nonoverlapping transcriptional responses. *Cell*, **126**, 467–475.

Nemhauser, J.L. *et al*. (2004) Interdependency of brassinosteroid and auxin signaling in Arabidopsis. *PLoS Biol.*, **2**, E258.

Osmont,K.S. *et al*. (2007) Hidden branches: developments in root system architecture. *Annu. Rev. Plant Biol.*, **58**, 93–113.

Pandey,S. *et al*. (2010) Boolean modeling of transcriptome data reveals novel modes of heterotrimeric G-protein action. *Mol. Syst. Biol.*, **6**, 372.

Philippi,N. *et al*. (2009) Modeling system states in liver cells: survival, apoptosis and their modifications in response to viral infection. *BMC Syst. Biol.*, **3**, 97.

Sabatini,S. *et al*. (1999) An auxin-dependent distal organizer of pattern and polarity in the Arabidopsis root. *Cell*, **99**, 463–472.

Sanchez-Corrales,Y.E. *et al*. (2010) The Arabidopsis thaliana flower organ specification gene regulatory network determines a robust differentiation process. *J. Theor. Biol.*, **264**, 971–983.

Sauer,M. *et al*. (2006) Canalization of auxin flow by Aux/IAA-ARF-dependent feedback regulation of PIN polarity. *Genes Dev*., **20**, 2902–2911.

Savaldi-Goldstein,S. *et al*. (2007) The epidermis both drives and restricts plant shoot growth. *Nature*, **446**, 199–202.

Scacchi,E. *et al*. (2009) Dynamic, auxin-responsive plasma membrane-to-nucleus movement of Arabidopsis BRX. *Development*, **136**, 2059–2067.

Scacchi,E. *et al*. (2010) Spatio-temporal sequence of cross-regulatory events in root meristem growth. *Proc. Natl Acad. Sci. USA*, **107**, 22734–22739.

Scheres,B. and Xu,J. (2006) Polar auxin transport and patterning: grow with the flow. *Genes Dev*., **20**, 922–926.

Sibout,R. *et al*. (2006) Opposite root growth phenotypes of hy5 versus hy5 hyh mutants correlate with increased constitutive auxin signaling. *PLoS Genet.*, **2**, e202.

Strader,L.C. *et al*. (2008) The IBR5 phosphatase promotes Arabidopsis auxin responses through a novel mechanism distinct from TIR1-mediated repressor degradation. *BMC Plant Biol.*, **8**, 41.

Tiwari,S.B. *et al*. (2003) The roles of auxin response factor domains in auxin-responsive transcription. *Plant Cell*, **15**, 533–543.

Trigueros,M. *et al*. (2009) The NGATHA genes direct style development in the Arabidopsis gynoecium. *Plant Cell*, **21**, 1394–1409.

Tromas,A. *et al*. (2009) The AUXIN BINDING PROTEIN 1 is required for differential auxin responses mediating root growth. *PLoS ONE*, **4**, e6648.

Vert,G. *et al*. (2005) Molecular mechanisms of steroid hormone signaling in plants. *Annu. Rev. Cell. Dev. Biol.*, 21, 177-201.

Vert,G. *et al*. (2008) Integration of auxin and brassinosteroid pathways by Auxin Response Factor 2. *Proc. Natl Acad. Sci. USA*, **105**, 9829–9834.

Vieten,A. *et al*. (2005) Functional redundancy of PIN proteins is accompanied by auxin-dependent cross-regulation of PIN expression. *Development*, **132**, 4521–4531.

Wang,S. *et al*. (2005) AUXIN RESPONSE FACTOR7 restores the expression of auxin-responsive genes in mutant Arabidopsis leaf mesophyll protoplasts. *Plant Cell*, **17**, 1979–1993.

Weijers,D. *et al*. (2005) Developmental specificity of auxin response by pairs of ARF and Aux/IAA transcriptional regulators. *EMBO J.*, **24**, 1874–1885.

Wisniewska,J. *et al*. (2006) Polar PIN localization directs auxin flow in plants. *Science*, **312**, 883.

Wittmann,D.M. *et al*. (2009) Transforming Boolean models to continuous models: methodology and application to T-cell receptor signaling. *BMC Syst. Biol.*, **3**, 98.